

Band Structure and Molecular Orientation of Ultrathin Epitaxial Films of Squaric Acid

Toshihiro Shimada,^{*,†} Hirotoshi Taira,[†] Tetsuhiko Miyadera,[†] Atsushi Koma,[†] and Koichiro Saiki[‡]

Department of Chemistry and Graduate School of Frontier Sciences, The University of Tokyo, Bunkyo-ku, Tokyo, 113-0033, Japan

Received: August 24, 2003; In Final Form: January 23, 2004

Ultraviolet photoelectron spectroscopy of epitaxial films of squaric acid ($\text{H}_2\text{C}_4\text{O}_4$), a two-dimensional antiferroelectric organic material, is reported. The band structure parallel to the two-dimensional molecular plane was derived, in which the dispersion of the HOMO-2 band was found to be as large as 0.7 eV. The molecular orientation was estimated by analyzing the angular distribution of the photoelectron intensities from various molecular orbitals using independent atomic center approximation.

Introduction

Squaric acid ($\text{H}_2\text{C}_4\text{O}_4$, SQ) is a two-dimensional molecular antiferroelectric material,^{1–5} and it has been studied as a model system of quantum paraelectricity.^{6,7} The dielectric phase transition is involved with delocalization of hydrogen atoms between adjacent molecules, and it is expected to be sensitive to the intermolecular distance and bond orientation. This material is also one of the simplest systems to study the interaction between π electrons and hydrogen bonding, which is a subject of intensive study in synthetic solid-state chemistry.^{8–10} Recently, we have found that SQ films can be grown epitaxially on alkali-halide surfaces with a certain range of lattice constants.¹¹ On those substrates, the lattice constants of the SQ films can be modified through the pseudomorphic growth when the film thickness is small enough. It makes this materials system suitable to study the effect of lattice distortion to the physical properties through “epitaxial pressure”¹¹ or “epitaxial strain”^{12–14} effects. It is important to determine the mutual molecular orientation because the antiferroelectric phase transition and the interplay between the π electrons and hydrogen bonding are strongly influenced by the geometry around hydrogen bonding.

In this paper, we report angle-resolved ultraviolet photoelectron spectroscopy (ARUPS) of SQ epitaxial films for the basis to elucidate those issues. As for the study of interaction between hydrogen bonding to the electronic structure, the band structure must be determined. ARUPS can be used to determine the band dispersion from the angular dependence of binding energies. In addition, it is also possible to apply ARUPS to estimate the molecular orientation. Although electron diffraction can be used to determine the lattice parameter in principle, it is rather difficult to apply it to determine the molecular orientation in thin films because of the large Debye–Waller-type decay induced by disorders. ARUPS data can be used to analyze the molecular orientation by comparing them with theoretically calculated angular dependence of photoelectron intensities.^{15–20}

The substrate for the epitaxy of SQ in this study was KCl(001), which has the lattice constant (0.629 nm) closest to that of SQ (0.614 nm) among pure alkali halides. Since KCl is an

insulator, we have used successive epitaxial growth of different alkali halide thin films on a conductive substrate to prepare a KCl(001) surface in order to prevent charging-up during the ARUPS measurements.^{21–24}

Experimental Section

SQ was grown by molecular-beam epitaxy on a heterostructured epitaxial substrate KCl(001)/NaCl(001)/GaAs(001), from which a single crystalline KCl can be formed on the conductive GaAs substrates.^{23,24} GaAs(001) was chemically etched by successive treatment in $\text{H}_2\text{SO}_4/\text{H}_2\text{O}_2/\text{H}_2\text{O} = 5:1:1$ (60 °C, 1 min) and 5:1:40 (RT, 20 s) solutions and further cleaned by heating (500 °C) in an ultrahigh vacuum. KCl and NaCl were evaporated from Knudsen cells by heating at ~ 700 –800 °C. The thickness of the films was monitored by a quartz crystal microbalance. The sample was kept at 150 °C, and the thickness of KCl and NaCl was 70 nm each. SQ was used as purchased (Aldrich) and introduced into the growth chamber using a load-lock mechanism. It was evaporated from a Knudsen cell by heating it at 140 °C. The growth rate was 0.1 nm/min, and the final thickness of the SQ film was 3 nm. The substrate was kept at room temperature during the growth. The crystallinity of the grown materials was monitored by reflection high-energy electron diffraction (RHEED) using signal amplification by a microchannel plate.²⁵ It was essential to reduce the RHEED probing electron current for observing the grown film because organic molecules are easily damaged by electron bombardment. After the growth of SQ, the sample was transferred to the analysis chamber. ARUPS was measured by ADES-500 (Vacuum Generators) using a He discharge lamp ($h\nu = 40.8$ eV (He–II)).

Results

Figure 1 shows RHEED patterns during the formation of the heterostructured sample. Streak patterns corresponding to the grown materials were observed as shown in Figure 1, which shows the epitaxial growth at each stage. The crystallinity of SQ was the same as that grown on bulk KCl single crystal, judging from the sharpness of the streaks and the azimuthal distribution of RHEED patterns.

No charging up was observed during the ARUPS measurement. Parts a and b of Figure 2 show the ARUPS ($h\nu = 40.8$

* To whom correspondence may be addressed. E-mail: shimada@chem.s.u-tokyo.ac.jp.

[†] Department of Chemistry, The University of Tokyo.

[‡] Graduate School of Frontier Sciences, The University of Tokyo.

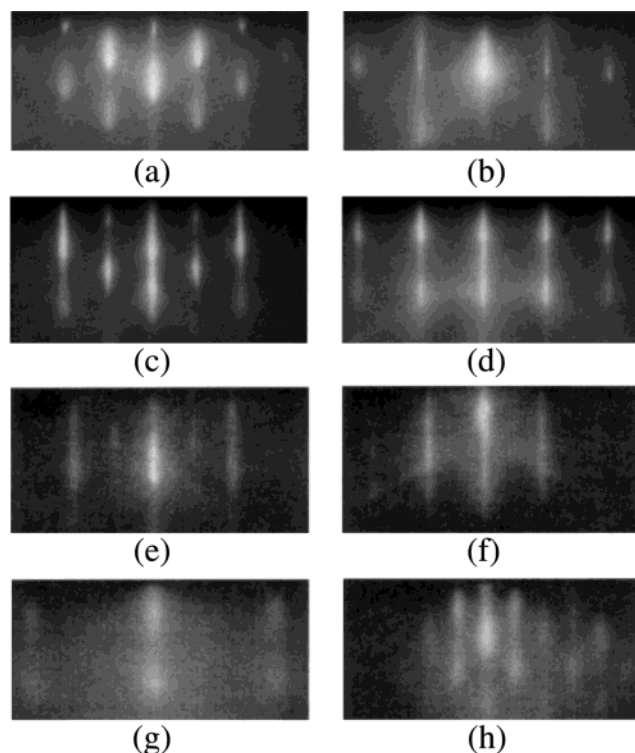


Figure 1. RHEED images taken at each stage of the sample preparation: (a) and (b) GaAs(001), (c) and (d) NaCl/GaAs, (e) and (f) KCl/NaCl/GaAs, (g) and (h) SQ/KCl/NaCl/GaAs. The incident azimuths are (a), (c), (e), (g) // [100] and (b), (d), (f), (h) // [110].

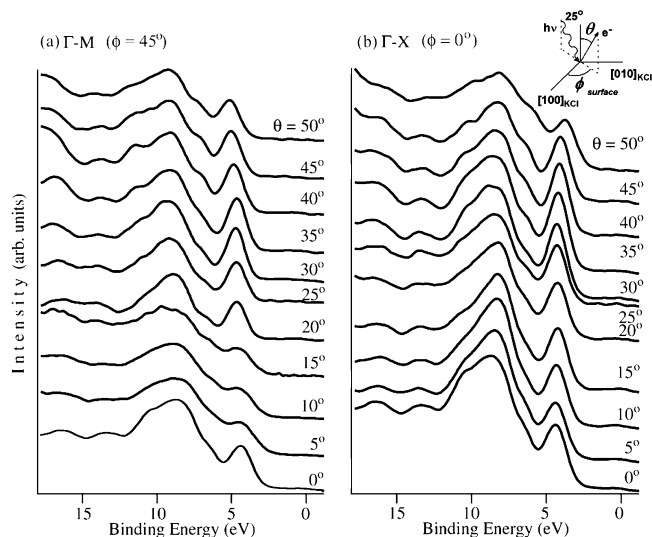


Figure 2. ARUPS of a SQ epitaxial film (3 nm thick) grown on a KCl/NaCl/GaAs(001) heteroepitaxial substrate.

eV) measured by changing the polar angles (θ) of electron emission along (a) [110] (Γ -M) and (b) [100] (Γ -X) of the substrates. The ultraviolet photons were irradiated along 25° off from the surface normal. UPS of the substrate (KCl/NaCl/GaAs) shows peak positions and shapes totally different from SQ films, and the contribution from the substrate to Figure 2 seems negligible. There is a large dip at binding energy $E_B = \sim 5.5$ eV. We name the regions $2.5 < E_B < 5.5$ and $5.5 < E_B < 12$ eV as regions I and II, respectively. When the polar angle of the electron spectrometer was changed, the peaks changed their binding energies and the relative intensities as seen in Figure 2.

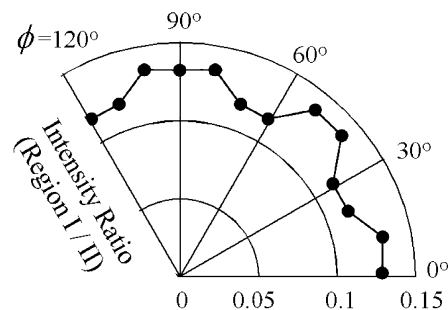


Figure 3. Azimuthal distribution of the intensity ratio (region I/region II). The electron emission polar angle (θ) is 65° .

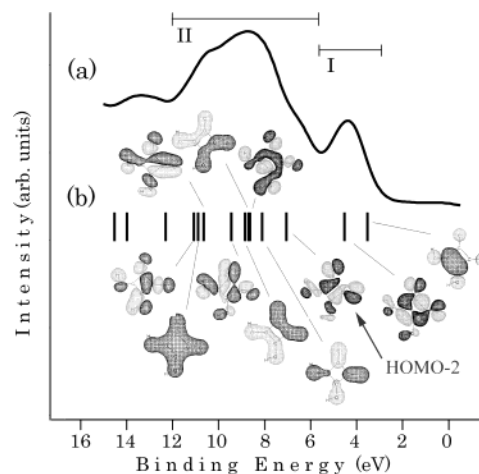


Figure 4. (a) UPS ($\theta = 0^\circ$), (b) energy levels and shapes of wave functions of a SQ molecule calculated by MNDO calculation.

We also measured the azimuthal distribution of the ARUPS peak intensities by changing the azimuthal angle (ϕ) and keeping $\theta = 65^\circ$. This value of θ was chosen because the difference of the relative intensity seemed large in a rough scan. To avoid the error in the normalization, we have calculated the ratio of the intensity of region I to region II. It is plotted as a function of the azimuth of the photoelectron detector in Figure 3, and 4-fold symmetry was observed. This symmetry is explained by the multidomain structure of the film. Although the room-temperature structure of the SQ crystal is monoclinic, there are eight equivalent ways to put the crystal on the surface with 4-fold symmetry, which comes from the combination of 4-fold rotation and mirror operation about the molecular plane. Since the angular distribution of the photoelectron is the summation of the signals from these eight equivalent domains, it is reasonable that 4-fold symmetry was observed.

Discussions

First we assign the UPS peaks by using molecular orbital calculations. Figure 4 shows the experimental spectrum ($\theta = 0^\circ$) and the energy levels derived by semiempirical modified neglect of diatomic overlap (MNDO) method. The shapes of wave functions corresponding to each energy level are illustrated in the figure. The experiment and the calculation agree well, and it was found that regions I and II consist of two and nine levels, respectively. The MNDO energies are shifted by a constant value (6.0 eV) so as to adjust the HOMO level with the experimental value because they may be different by a certain value from the calculated values due to the final-state effect. The energies show good agreement with the experimental peak energies that were determined by taking the second derivative of the spectra.

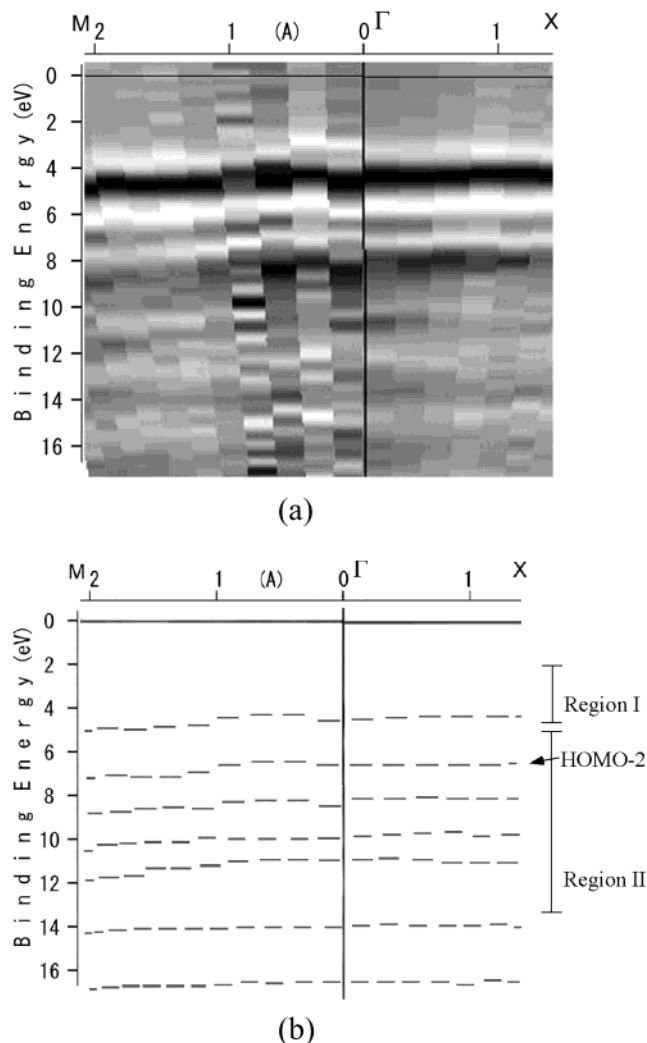


Figure 5. Band dispersion of SQ derived from ARUPS shown in Figure 2. (a) Second derivative of ARUPS plotted in gray scale. The dark part corresponds to the larger density of states. (b) Peak positions extracted from (a).

The binding energies of the peaks in the ARUPS spectra correspond to the band dispersion of SQ. Since the structure of SQ is two-dimensional with π electrons parallel to the surface, the band dispersion along surface normal is expected to be weak. Therefore two-dimensional band structure parallel to the surface can be derived from the UPS measurement by changing the polar angle θ of the electron detector (Figure 2). The momentum–energy (k – E) relationship was obtained from the UPS spectra as shown in Figure 5. They have been constructed from the experimental energy distribution curves collected for many different angles. Momentum was calculated according to the equation $k = ((2m/\hbar^2)E_k)^{1/2} \sin \theta$, in which E_k is kinetic energy of electron. The gray-scale intensity was derived from the second derivative of the spectra with respect to the electron binding energy.

From the energy dispersion of k – E relationship, the width of each energy band can be determined. It is difficult to resolve the two peaks in region I, and we refrain from discussing dispersion in region I. The shallowest peak level in region II (HOMO-2) is well resolved and shows a dispersion of 0.7 eV. This value is among the largest values for intermolecular dispersion in typical molecular semiconductors (e.g., C_{60} (0.4 eV)²⁶ and BTQBT (0.7 eV)²⁷) but smaller than intramolecular ones or charge-transfer salts (e.g., alkyl chain^{28–32} or d– π

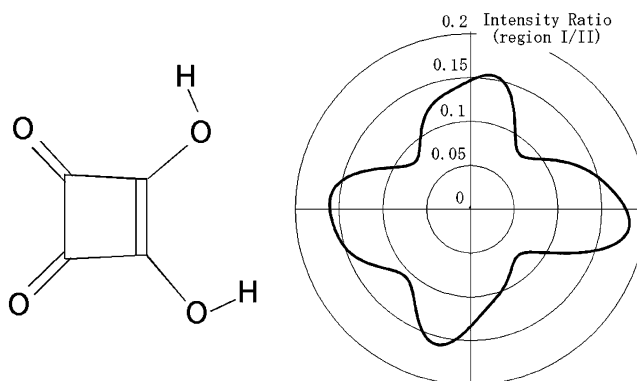


Figure 6. Azimuthal distribution of photoemission intensity ratio (region I/II) of SQ (for $h\nu = 40.8$ eV and $\theta = 65^\circ$) calculated with IAC approximation.

complex³³). The large dispersion is probably due to the π electron of the HOMO-2 level extended to the whole molecule, as seen in the illustration in Figure 4.

Next we analyze the azimuthal distribution of the ARUPS peak intensities shown in Figure 3, which is related with the molecular orientation within a unit lattice. The angular distribution of the intensity of the photoelectrons comes from the interference of the photoelectrons emitted from a molecular orbital. Although there are various degrees of approximation to calculate the interference effects, independent atomic center (IAC) approximation is widely used to determine the molecular orientation.^{15–20} In brief, azimuthal distribution of the photoelectron intensity ratio is given by taking into account the interference of the emitting electron waves. In this approximation, it is assumed that photoelectrons are emitted independently from the center of the atoms constituting the molecule. The initial and final states are approximated by linear combination of spherical harmonic atomic orbitals. The coefficients of the linear combinations are given by the molecular orbital calculation as shown in Figure 4. The matrix elements for the photoelectron emission are calculated from that of each atomic orbital considering the phase shifts in the excitation of atomic orbitals.

We used the molecular wave functions obtained from MNDO calculation (Figure 4). By use of the amplitude and the phase of the wave function at each atom and the matrix element parameters which were calculated by the scheme derived by Goldberg et al.,²⁰ the azimuthal distribution of photoelectron intensity ratio of region I/region II is calculated and plotted in Figure 6. Here we assumed that the molecules lie flat on the surface because the calculated azimuthal distribution was insensitive to the tilt of the molecule by small angles ($\leq 10^\circ$). It is expected that the azimuthal rotation α of the molecules from the main axis of the substrate lattice (Figure 7 left) can be obtained by comparing the experimental result with the calculation. From the symmetry of the molecule and the substrate surface, there should be 4-fold rotational and mirror symmetry in the azimuthal distribution. By least-squares fitting of the symmetric sum of azimuthally rotated curve of Figure 6 to the intensity ratio shown in Figure 3, α was determined to be $22.3 \pm 1.4^\circ$. In Figure 7, the symmetric sums for other values of α are also shown for comparison. This value of α is close to that reported for the bulk crystal of SQ ($22.35 \pm 0.08^\circ$ at 292 K, 2.75 GPa;³⁴ $21.90 \pm 0.01^\circ$ at 394 K, 1 atm³⁵). This result indicates that the molecular orientation in an ultrathin epitaxial film was the same as that of bulk crystal of SQ and that the two-dimensional structure of the material is maintained.

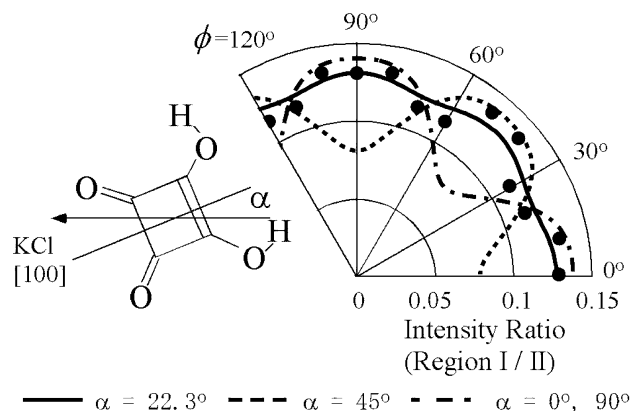


Figure 7. Azimuthal distribution of the intensity ratio of region I/region II. ● represent experiment (same as Figure 3). Lines represent calculated intensity ratios for various molecular orientation (angle α in the inset) using the result of IAC approximation shown in Figure 6 and symmetry consideration. Solid line, $\alpha = 22.3^\circ$ (best fit); broken line, $\alpha = 45^\circ$; dash-dotted line, $\alpha = 0^\circ$. $\alpha = 90^\circ$ gives the same result with $\alpha = 0^\circ$.

Conclusion

ARUPS of an epitaxial SQ film has been measured and analyzed. An epitaxial KCl film grown by successive heteroepitaxy has been used as the substrate to prevent charging-up during the measurement. Two-dimensional band dispersion of this closely associated π -electron system amounts to 0.7 eV in the HOMO-2 band, which is rather large as an intermolecular dispersion of organic materials. The molecular orientation in the film relative to the crystal axes of the substrate was determined from the azimuthal distribution of the UPS peak intensities compared with IAC approximation.

Acknowledgment. The present work was supported by Grants-in-Aid from MEXT and Matsuo Foundation. Funding from PRESTO-JST and NEDO(00B64026c) is also acknowledged.

References and Notes

- (1) Semmingsen, D. *Acta Chem. Scand.* **1973**, 27, 3961.
- (2) Semmingsen, D.; Feder, J. *Solid State Commun.* **1974**, 15, 1396.
- (3) Samuelson, E. J.; Semmingsen, D. *Solid State Commun.* **1975**, 17, 216.
- (4) Samuelson, E. J.; Semmingsen, D. *J. Phys. Chem. Solids* **1977**, 38, 1275.
- (5) Semmingsen, D.; Tun, Z.; Nelm, R. J.; McMullan, R. K.; Koetzle, T. F. *Kristallogr. Z.* **1995**, 210, 84.

- (6) Samara, G. A.; Semmingsen, D. *J. Chem. Phys.* **1979**, 71, 1401.
- (7) Moritomo, Y.; Tokura, Y.; Takahashi, H.; Mori, N. *Phys. Rev. Lett.* **1991**, 67, 2041.
- (8) Mitani, T.; Kitagawa, H.; Morii, K.; Yoshida, D.; Sakaim, K.; Itoh, T.; Nakatsuji, K. *Mol. Cryst. Liq. Cryst. A* **1996**, 285, 249.
- (9) Heuse, K.; Fourmigue, M.; Batail, P.; Canadell, E.; Auban-Senzier, P. *Chem.-Eur. J.* **1999**, 5, 2971.
- (10) Gervasio, F. L.; Carioni, P.; Parrinello, M. *Phys. Rev. Lett.* **2002**, 89, 108102.
- (11) Shimada, T.; Taira, H.; Koma, A. *Chem. Phys. Lett.* **1998**, 291, 419.
- (12) Locquet, J.-P.; Perret, J.; Fompeyrine, J.; Machler, E.; Seo, J. W.; Van Tendeloo, G. *Nature* **1998**, 394, 453.
- (13) Scholl, A.; Stohr, J.; Kining, J.; Seo, J. W.; Fompeyrine, J.; Siegwart, H.; Locquet, J.-P.; Nolting, F.; Anders, S.; Fullerton, E. E.; Scheinfein, M. R.; Padmore, H. A. *Science* **2000**, 287, 1014.
- (14) Tiwari, A.; Jin, C.; Narayan, J. *Appl. Phys. Lett.* **2002**, 80, 4039.
- (15) Grobman, W. D. *Phys. Rev. B* **1978**, 17, 4573.
- (16) Hasegawa, S.; Tanaka, S.; Yamashita, Y.; Inokuchi, H.; Fujimoto, H.; Kamiya, K.; Seki, K.; Ueno, N. *Phys. Rev. B* **1993**, 48, 2596.
- (17) Kawaguchi, T.; Tada, H.; Koma, A. *J. Appl. Phys.* **1994**, 75, 1486.
- (18) Kawaguchi, T.; Tada, H.; Koma, A. *Appl. Phys. A* **1995**, 61, 631.
- (19) Ueno, N.; Suzuki, K.; Hasegawa, S.; Kamiya, K.; Seki, K.; Inokuchi, H. *J. Chem. Phys.* **1993**, 99, 7169.
- (20) Goldberg, S. M.; Fadley, C. S.; Kono, S. *J. Electron. Spectrosc. Relat. Phenom.* **1981**, 21, 285.
- (21) Yang, M. H.; Flynn, C. P. *Phys. Rev. Lett.* **1989**, 62, 2476.
- (22) Yang, M. H.; Flynn, C. P. *Phys. Rev. B* **1990**, 41, 8500.
- (23) Nakamura, Y.; Saiki, K.; Koma, A. *J. Vac. Sci. Technol. A* **1992**, 10, 321.
- (24) Saiki, K.; Nakamura, Y.; Nishida, N.; Gao, W.; Koma, A. *Surf. Sci.* **1994**, 301, 29.
- (25) Saiki, K.; Kono, T.; Ueno, K.; Koma, A. *Rev. Sci. Instrum.* **2000**, 71 (9), 3478.
- (26) Gensterblum, G.; Preaux, J. J.; Thiry, P. A.; Caudao, R.; Buslaps, T.; Johnson, R. L.; Le Lay, G.; Aristov, V.; Gunther, R. *Phys. Rev. B* **1993**, 48, 14756.
- (27) Fujimoto, H.; Kamiya, K.; Tanaka, S.; Mori, T.; Yamashita, Y.; Inokuchi, H. *Chem. Phys.* **1992**, 165, 135.
- (28) Seki, K.; Karlsson, U. O.; Engelhardt, R.; Koch, E. E. *Chem. Phys. Lett.* **1984**, 103, 343.
- (29) Seki, K.; Ueno, N.; Karlsson, U. O.; Engelhardt, R.; Koch, E. E. *Chem. Phys.* **1986**, 105, 247.
- (30) Ueno, N.; Gaedeke, W.; Koch, E. E.; Engelhardt, R.; Dudde, R.; Laxhuber, L.; Moehwald, H. *J. Mol. Electron.* **1985**, 1, 19.
- (31) Fujimoto, H.; Mori, T.; Inokuchi, H.; Ueno, N.; Sugita, K.; Inokuchi, H. *Phys. Rev. B* **1990**, 41, 1176.
- (32) Ueno, N.; Seki, L.; Sato, N.; Fujimoto, H.; Sugita, K.; Inokuchi, H. *Phys. Rev. B* **1990**, 41, 1176.
- (33) Schmeisser, D.; Jaegermann, W.; Pottenkofer, Ch.; Wachtel, H.; Jimenez-Gonzales, A.; von Shutz, J. U.; Wolf, H. C.; Erk, P.; Meixner, H.; Hunig, S. *Solid State Commun.* **1992**, 81, 827.
- (34) Katrusiak, A.; Nelm, R. J. *J. Phys. C: Solid State Phys.* **1986**, 19, L765.
- (35) Hollander, F. J.; Semmingsen, D.; Koetzle, T. F. *J. Chem. Phys.* **1977**, 67, 4825.